ADVANCED FUNCTIONAL MATERIALS

Supporting Information

for *Adv. Funct. Mater.*, DOI: 10.1002/adfm.201303737

Magnetite Crystal Orientation in Magnetosome Chains

*André Körnig, Michael Winklhofer, Jens Baumgartner, Teresa Perez Gonzalez, Peter Fratzl, and Damien Faivre**

Supplementary Information

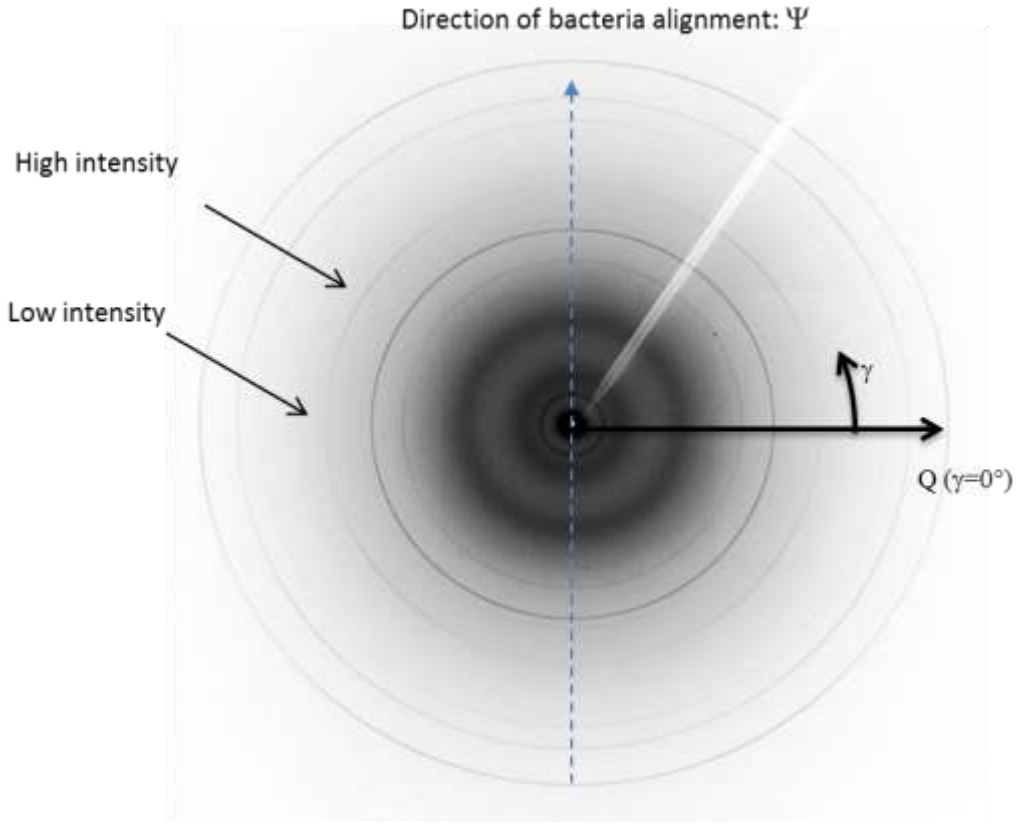

Supplementary Figure 1: Two dimensional diffraction pattern, darker pixel display higher diffracted intensity. The dashed line indicates the direction of the bacterial alignment along the external magnetic field. The solid lines indicate the direction of integration of the XRD pattern.

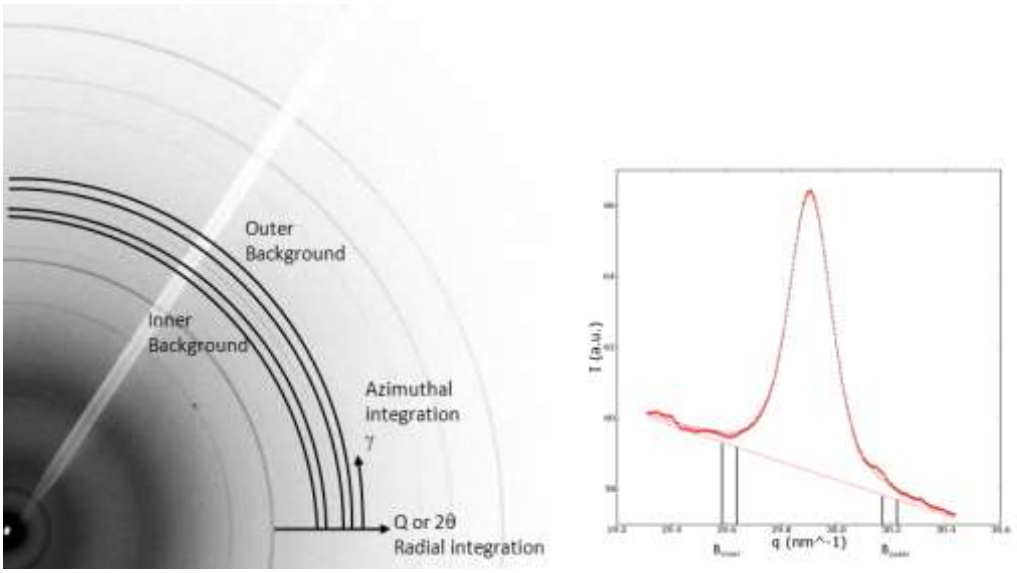

Supplementary Figure 2: Scheme of local background subtraction: 3 radial integrations are performed to obtain the signal.

Local background subtraction: First an azimuthal integration over γ was performed to obtain the $I(Q)$ profile of the plane. A linear and a pseudo-Voigt function were fitted to the profile to determine the peak position and the FWHM. The Q-range for the radial integration of the ring ($I_{ring}(\gamma) = \int_{Q_{min}}^{Q_{max}} I(Q,\gamma)dQ$), was then the center of the peak and a range of two times the *FWHM* as the width ($Q_{max} = Q_{peak} + FWHM$ and $Q_{min} = Q_{peak} - FWHM$). This range covers 98 % of the intensity peak. The range for the radial integration of the inner $B_{inner}(\gamma)$ and outer background $B_{outer}(\gamma)$ was 2 detector pixels wide and adjacent to the peak. With these 3 radial integrations, the inner background, the outer background and the ring itself, the azimuthal intensity variation of a set of the planes $I_{hkl}(\gamma)$ can be derived as: $I_{hkl}(\gamma) = I_{ring}(\gamma) - \left[\frac{B_{outer}(\gamma) + B_{inner}(\gamma)}{2}\right]$

Supplementary Table 1: Overview of names used for the different angles and their definition:

γ	Azimuthal angle on the detector starting in the horizontal plane. The azimuthal intensity variations (AID) is a function of this angle
Ψ	Direction of the fiber axis, with respect to γ, starting in the horizontal plane
α	Measured angular difference between intensity maxima and direction of fiber axis
ρ	theoretical angle between two crystallographic directions
2θ	scattering angle with respect to the X-ray beam

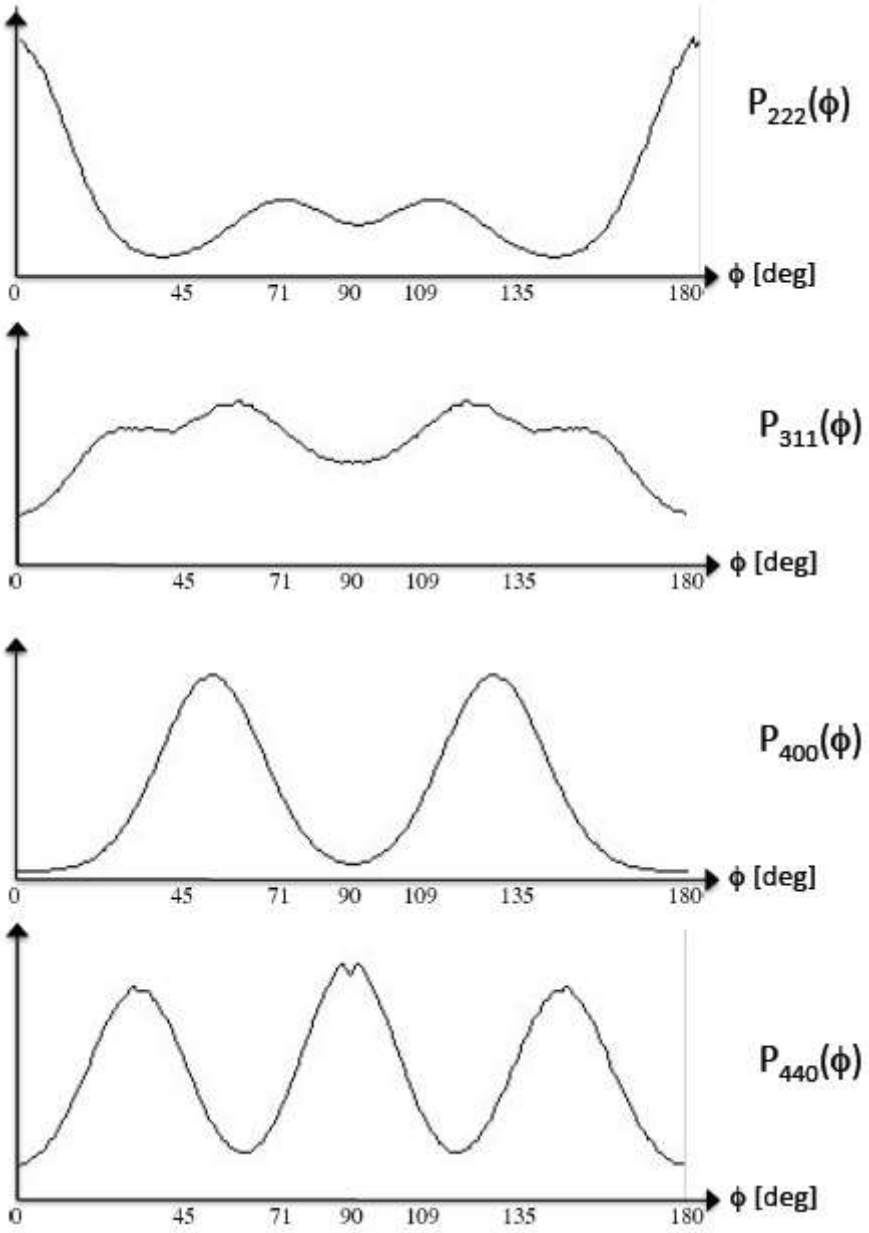

Supplementary Figure 3: Forward modeled AID of Debey rings for a 111 texture with a Gaussian kernel of 15deg HWHM, using the software package ANAELU [1]. There is good agreement between simulated and experimental AIDs (Fig. 4 and Fig 5a-c).

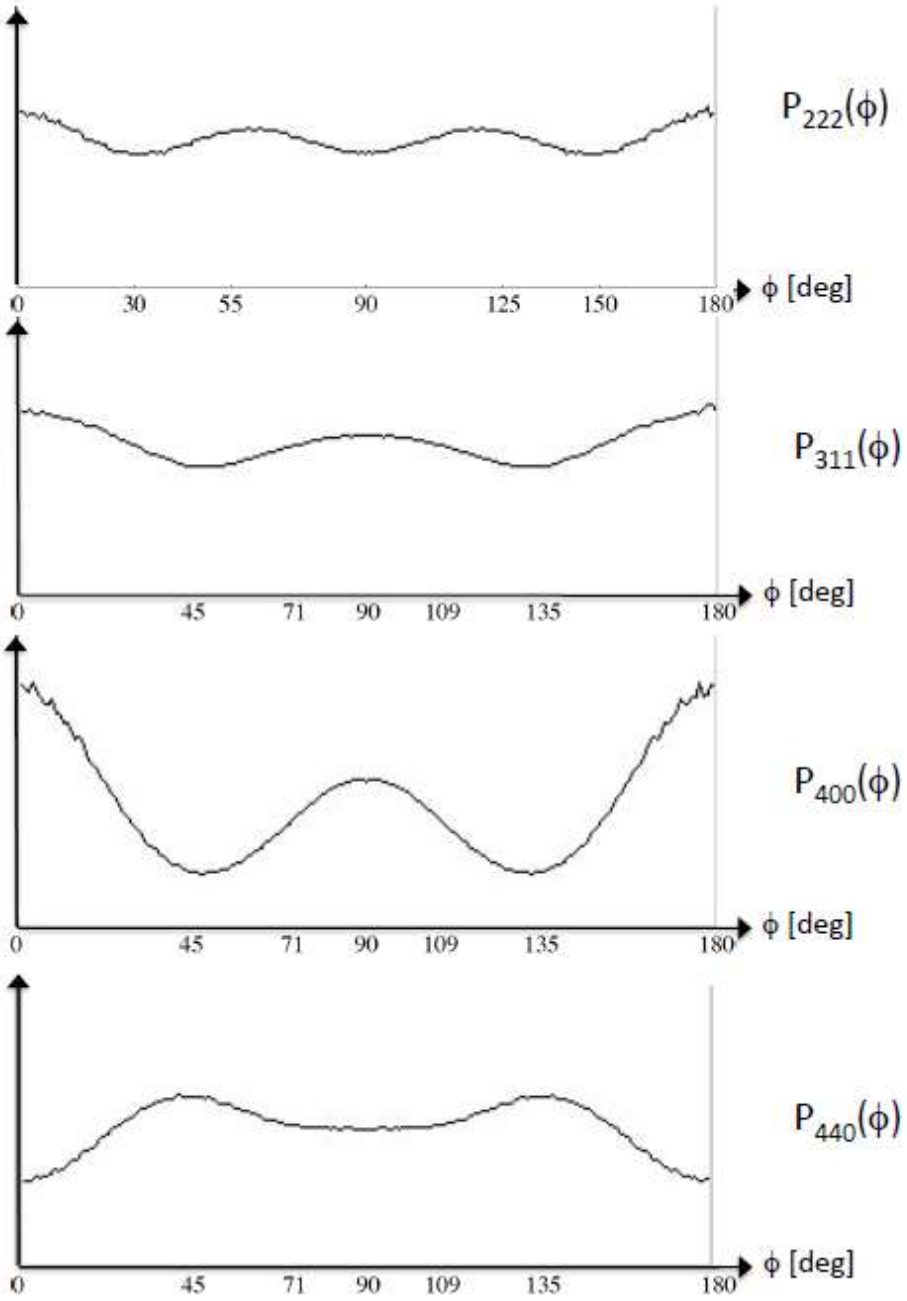

Supplementary Figure 4: Forward modeled AID of Debey rings for a 100 texture with a Gaussian kernel of 25deg HWHM, using the software package ANAELU [1]. There is good agreement between simulated and experimental AIDs (Fig 5d for RS-1). The AID for the 222 lattice reflection is shown for the sake of completeness.

Modelling of competing anisotropies

Typically, magnetite magnetosomes with regular morphology (cubo-octahedra, hexagonal prisms) are elongated along a crystallographic <111> axis, with the elongation oriented along the chain axis [2-6]. In magnetosomes with less symmetric shapes (e.g., "tooth shaped"), the axis of elongation may be <100>, <114>, or <112> [7-12].

The <111> directions are magnetic easy directions in magnetite, which is why elongation along a particular <111> axis favors the equilibrium magnetization to be coaxial with the elongation. In contrast, for the example of elongation along a magnetic hard <100> axis, as in RS-1, the shape anisotropy due to elongation along <100> competes with the easy <111> axis and deflects the equilibrium magnetization away from a <111> direction towards the axis of elongation. To determine the angle θ between the equilibrium magnetization vector and the elongation axis for a magnetosome with mixed cubic and uniaxial shape anisotropy, we minimize the following expression for the anisotropy energy (per unit volume),

$$e_{an} = K_1(\alpha_1^2\alpha_2^2 + \alpha_2^2\alpha_3^2 + \alpha_3^2\alpha_1^2) - K_u(h\alpha_1 + k\alpha_2 + l\alpha_3)^2 + \\ -\mu_0 H M_s(\beta_1\alpha_1 + \beta_2\alpha_2 + \beta_3\alpha_3), \qquad (1)$$

(e.g. [13]). The first term is the intrinsic cubic magnetocrystalline anisotropy in first order, where K_1 is the first magnetocrystalline anisotropy constant and the α_i are the Cartesian component of the direction of the magnetization, where both are defined with respect to the cubic <100> system, say the [001] direction. The second term is the shape induced uniaxial anisotropy, where the *h, k,* and l are the (normalized, i.e., $h^2 + k^2 + l^2 = 1$) Miller indices of the direction of the elongation, and $K_u = \Delta N K_d$ is the uniaxial anisotropy energy constant, where ΔN is the effective demagnetization factor and $K_d = \frac{\mu_0}{2} M_s^2$ is the stray-field energy constant and M_s is the saturation magnetization (480 kA/m for magnetite). The third term is the Zeemand field energy due to an external magnetic field of strength *H*, where β_i are the Cartesian components of the direction of the field.

For elongation and applied field along $[hkl] = [001]$, $K_1 = -|K_1|$ (since $K_1 < 0$ for magnetite), and ΔN >0 (for a prolate body), Eq. (1) becomes

$$\frac{e_{an}}{QK_d} = \frac{3}{4}\alpha_3^4 - \left(\frac{\Delta N}{Q} + \frac{1}{2}\right)\alpha_3^2 - \frac{b}{Q}\alpha_3 - \frac{1}{4}, \qquad (2)$$

where $Q = |K_1|/K_d$, $b = \frac{2H}{M_s}$, and $\alpha_3^2 = \cos^2\theta$.

For H =0, an analytical solution to the minimization problem is readily obtained as

$$\alpha_3^2 = \frac{1 + \frac{2\Delta N}{Q}}{3}, \qquad (3)$$

for $0 \le \Delta N < Q$. For $\Delta N \ge Q$, $\alpha_3^2 = 1$, i.e., the magnetization is along [001]. For magnetite at room temperature, $Q = 0.08$, and the critical demagnetization factor above which the [001] axis becomes the easy axis is given by $\Delta N^{crit} = 0.08$, which for a prolate ellipsoid of revolution corresponds to a critical aspect ratio of 1.23 (long axis/short axis). For a prism with square cross section, $\Delta N^{crit} = 0.08$ is equivalent to an aspect ratio of 1.29. The observed elongations in RS-1 (see Fig. 5b in [10]) exceed these values.

The external field can no longer be neglected if *b* (in reduced units) is of the order of *Q* (i.e., if $H \sim \frac{QM_s}{2}$ or, in practical units, 24 mT). When applied along the axis of such a chain, the external reduces the critical aspect ratio by b/(2Q), i.e., $\Delta N^{crit} = Q - \frac{b}{2Q}$., see Fig. 1. Likewise, if the particle spacing is small and the axes of elongations are oriented along the chain axis, then intra-chain magnetostatic interactions increase the effective ΔN so that the critical condition can be satisfied

for smaller aspect ratios. This is similar to the action of an external field applied along the chain direction.

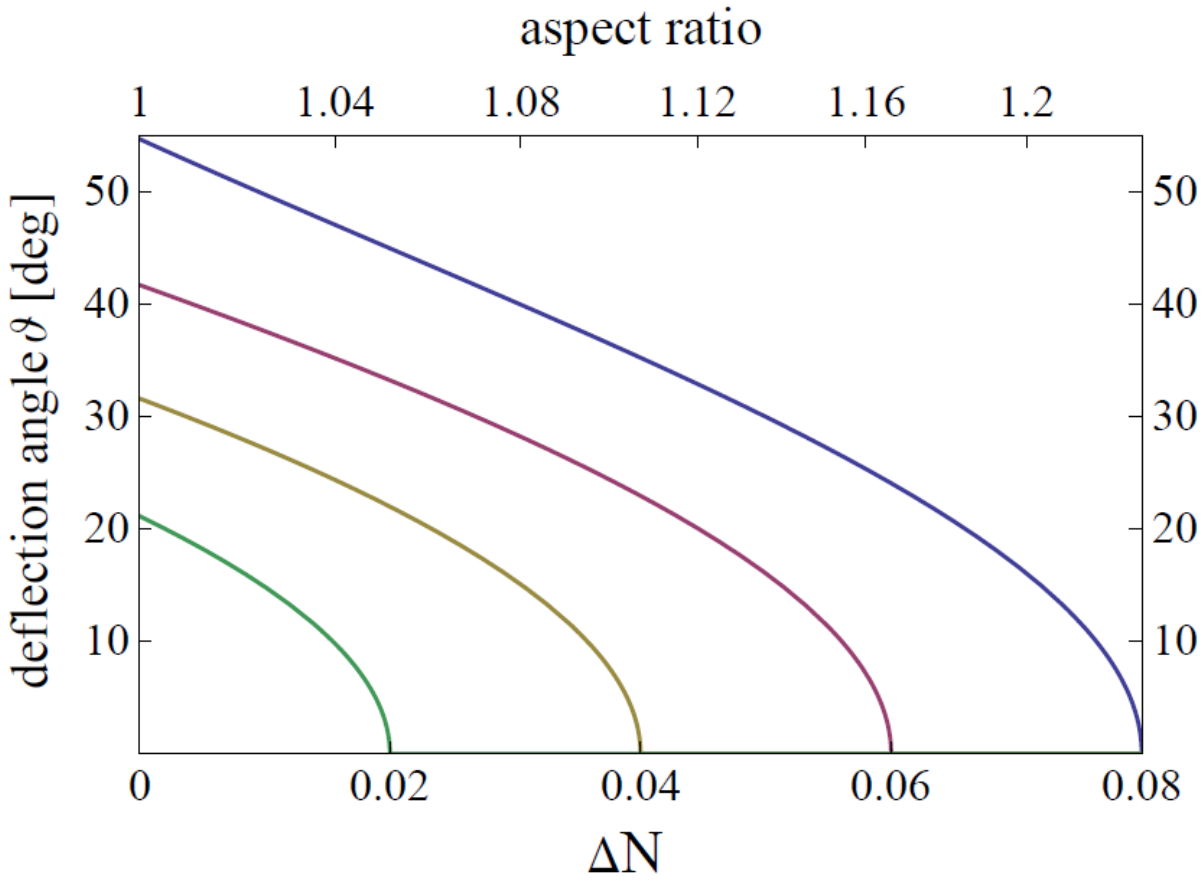

Supplementary Figure 5: Deflection angle θ for the situation of a single-domain magnetite particle ($\mathbf{Q = 0.08}$) elongated along a [001] in function of the effective demagnetization factor ΔN (bottom abscissa) or aspect ratio (top abscissa), for zero external field (blue) and external field applied along [001] (magenta: 12 mT, yellow: 24 mT, green: 36 mT).

Calculation of the angle ρ for different [111] and [100] fiber texture

From equation $\cos\rho = \frac{uh + vk + wl}{\sqrt{u^2 + v^2 + w^2} \cdot \sqrt{h^2 + k^2 + l^2}}$ the angle between the normal of a set of planes {hkl} and the crystallographic direction [uvw] can be calculated. The second left column in the first table shows the r values with respect to [111] direction: Respecting the angle of the direction of the fiber axis Ψ, a certain ρ value results in 4 γ angles, where a higher intensity can be expected: γ=Ψ+ ρ, γ= Ψ − ρ, γ = Ψ+180°+ ρ and γ = Ψ+180°− ρ:

For a [111] alignement with and Ψ=92° (MSR-1):

Planes {hkl}	For [111] Angle ρ		γ	γ	γ	γ
222	0,0		92	272	272	
	70,5		162,53	201,47	342,53	21,47
200/400	54,7		146,74	217,26	326,74	37,26
220/440	35,3		127,26	236,74	307,26	56,74
	90,0		182	182	2	2
311	29,5		121,5	242,5	301,5	62,5
	58,5		150,52	213,48	330,52	33,48
	80,0		171,98	192,02	351,98	12,02

For a 100 alignment of the crystals as in the RS-1 sample with Ψ = 95° the values are :

plane	For [100] Angle ρ		γ	γ	γ	γ
200/400	0		95	275	275	95
	90		185	185	5	5
222	54,7		149,74	220,26	329,74	40,26
220&440	45		140	230	320	50

	90		185	185	5	5
311	25,2		120,24	249,76	300,24	69,76
	72,45		167,45	202,55	347,45	22,55

Supplementary references

[1] L. Fuentes-Montero, M. E. Montero-Cabrera, L. Fuentes-Cobas, J. Appl. Cryst. 2011, 44, 241.
[2] T. Matsuda, J. Endo, N. Osakabe, A. Tonomura, T. Arii, Nature 1983, 302, 411.
[3] S. Mann, R. B. Frankel, R. P. Blakemore, Nature 1984, 310, 405.
[4] P. R. Buseck, R. E. Dunin-Borkowski, B. Devouard, R. B. Frankel, M. R. McCartney, P. A. Midgley, M. Pósfai, M. Weyland, Proc. Natl. Acad. Sci. U.S.A. 2001, 98, 13490.
[5] U. Lins, M. R. McCartney, M. Farina, R. B. Frankel, P. R. Buseck, Appl. Environ. Microbiol. 2005, 71, 4902.
[6] L. G. Abracado, F. Abreu, C. N. Keim, A. P. C. Campos, U. Lins, M. Farina, Phys. Biol. 2010, 7, 046016.
[7] A. P. Taylor, J. C. Barry, R. I. Webb, J. Microsc. 2001, 201, 84.
[8] M. Hanzlik, M. Winklhofer, N. Petersen, J. Magn. Magn. Mater. 2002, 248, 258.
[9] T. Kasama, M. Pósfai, R. K. K. Chong, A. P. Finlayson, P. B. Buseck, R. B. Frankel, R. E. Dunin-Borkowski, Am. Mineral. 2006, 91, 1216.
[10] M. Pósfai, B. M. Moskowitz, B. Arato, D. Schüler, C. Flies, D. A. Bazylinski, R. B. Frankel, Earth Planet. Sci. Lett. 2006, 249, 444.
[11] U. Lins, C. N. Keim, F. F. Evans, M. Farina, P. R. Buseck, Geomicrobiol. J. 2007, 24, 43.
[12] J. H. Li, Y. X. Pan, Q. S. Liu, Y. Z. Kui, N. Menguy, R. C. Che, H. F. Qin, W. Lin, W. F. Wu, N. Petersen, X. A. Yang, Earth Planet. Sci. Let. 2010, 293, 368.
[13] D. G. Tonge, E. P. Wohlfarth, Phil. Mag. 1958, 3, 536.